



HAL
open science

Molecular mass effect on the flow of a thermal binary gas mixture in a circular micro channel

Cédric Croizet, R. Gagnol

► **To cite this version:**

Cédric Croizet, R. Gagnol. Molecular mass effect on the flow of a thermal binary gas mixture in a circular micro channel. 31ST INTERNATIONAL SYMPOSIUM ON RAREFIED GAS DYNAMICS: RGD31, Jul 2018, Glasgow, United Kingdom. pp.160002, 10.1063/1.5119649 . hal-02302275

HAL Id: hal-02302275

<https://hal.science/hal-02302275>

Submitted on 12 Oct 2022

HAL is a multi-disciplinary open access archive for the deposit and dissemination of scientific research documents, whether they are published or not. The documents may come from teaching and research institutions in France or abroad, or from public or private research centers.

L'archive ouverte pluridisciplinaire **HAL**, est destinée au dépôt et à la diffusion de documents scientifiques de niveau recherche, publiés ou non, émanant des établissements d'enseignement et de recherche français ou étrangers, des laboratoires publics ou privés.

Molecular Mass Effect on the Flow of a Thermal Binary Gas Mixture in a Circular Micro Channel

C. Croizet^{a)} and R. Gatignol^{b)}

Sorbonne Université, CNRS, Institut Jean Le Rond d'Alembert, F-75005 Paris, France

^{a)}Corresponding author: cedric.croizet@sorbonne-universite.fr

^{b)}renee.gatignol@sorbonne-universite.fr

Abstract. Micro metric channels are present in a wide range of applications. For instance, micro filters are used in high-tech industry to detect biological or chemical entities as well as in daily-use objects. In order to describe the gas flows in the micro channels involved in these tools, Bird's DSMC method is frequently used. This method is efficient but it requires a large computation time to obtain a flow description [1, 2]. Consequently, it is of main interest to develop alternative asymptotic models in order to predict these flows more quickly. The purpose of this communication is to model the flow of a mixture of two compressible gases in circular micro pipes with a wall temperature depending on the longitudinal space variable. This work deals with flows at low Mach numbers and at low to moderate Knudsen numbers that correspond to the slip-flow regime. Under these assumptions, it is suitable to use the usual macroscopic balance laws of mass, momentum and energy (Navier-Stokes-Fourier equations) with additional coupling terms in the momentum and energy equations [3, 4, 5, 6]. The results of this asymptotic modeling are compared to DSMC simulations in the same configuration. The effects of the molecular weights is investigated.

INTRODUCTION

Because of the increasing importance of sub-milimeter-sized devices in the every day life, a large number of works are devoted to the analysis of micro channel flows. In particular, various studies of gaseous flows in micro channels exist covering the theoretical, numerical and experimental aspects of these flows [1, 2, 7, 8, 9]. In a numerical point of view, Bird's DSMC is frequently used. This method is efficient but it requires a large computation time [1, 2]. As a consequence, the development of asymptotic models describing these flows is an interesting alternative. This approach has been used in the case of a single gas in [8, 10] for instance and for a gas mixture in plane [11, 6] or axisymmetrical [12, 5] channels.

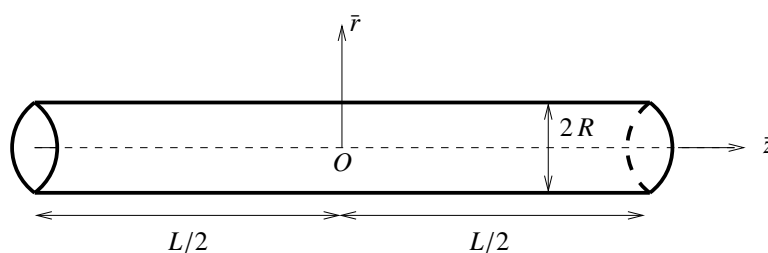


FIGURE 1. Geometry of the channel

In this contribution, we consider a cylindrical micro pipe ; its geometry is shown in Fig. 1. Driven by both temperature and pressure gradients, a mixture of two compressible gases flows in this micro channel. The temperature of the channel wall depends on the longitudinal space variable z . The aim is to model these micro-flows with a macroscopic approach and to obtain an asymptotic model for describing the main physical phenomena. We are interested in flows at low Mach numbers and at low to moderate Knudsen numbers that corresponds to the slip-flow

regime. Consequently, the movement equations are the usual macroscopic balance laws of mass, momentum and energy (Navier-Stokes-Fourier equations) with additional coupling terms in the momentum and energy equations [3, 4, 12]. In this weakly rarefied regime, the usual no-slip wall boundary conditions are replaced with slip conditions. In this paper, first order jump boundary conditions for the velocity and the temperature are written [8] at the walls. The flow is assumed to be axisymmetric and steady. At the circular channel inlet, each gas has its own pressure and velocity.

In the next section we present the model equations. In the following sections, an asymptotic analysis is made on the corresponding dimensionless equations. The small parameter is the aspect ratio of the channel. The solution at the first order is investigated and compared to DSMC simulations in the same configuration. Then, the asymptotic model is applied to analyze the effects of a wall constant temperature gradient and of the molecular masses on the flow. The last section is devoted to a short conclusion.

MODEL EQUATIONS

The micro channel has the length $L = 10 \mu\text{m}$ and the radius $R = 1 \mu\text{m}$ (Fig. 1). The channel wall at $\bar{r} = R$ is at rest and has a temperature depending on the longitudinal coordinate $\bar{T}_w(\bar{z})$. The movement equations are the Navier-Stokes-Fourier equations for a mixture of two ideal gases denoted with "a" and "b", with constant heat capacities c_{pa} and c_{pb} at constant pressure and c_{va} and c_{vb} at constant volume. The shear viscosities μ_a and μ_b and thermal conductivities κ_a and κ_b depend on the temperature only and are such as the Prandtl numbers are constant. The model equations are the usual balance equations with additional coupling terms. The "bars" are used for the quantities with dimension (except when they are constant) and removed to denote the associated dimensionless quantities. For the species a , we have the three following balance equations for the mass, the momentum and the energy:

$$\frac{\partial \bar{\rho}_a}{\partial \bar{t}} + \bar{\nabla} \cdot (\bar{\rho}_a \bar{\mathbf{u}}_a) = 0, \quad (1)$$

$$\frac{\partial}{\partial \bar{t}} (\bar{\rho}_a \bar{\mathbf{u}}_a) + \bar{\nabla} \cdot (\bar{\rho}_a \bar{\mathbf{u}}_a \bar{\mathbf{u}}_a - \bar{\sigma}_a) = \bar{v}_{ab} \bar{\rho}_a (\bar{\mathbf{u}}_a - \bar{\mathbf{u}}_a^*), \quad (2)$$

$$\frac{\partial}{\partial \bar{t}} \left(\frac{1}{2} \bar{\rho}_a \bar{\mathbf{u}}_a^2 + \bar{\rho}_a \bar{e}_a \right) + \bar{\nabla} \cdot \left[\bar{\rho}_a \left(\frac{1}{2} \bar{\mathbf{u}}_a^2 + \bar{e}_a \right) \bar{\mathbf{u}}_a - \bar{\sigma}_a \cdot \bar{\mathbf{u}}_a + \bar{\mathbf{q}}_a \right] = \bar{S}_a^E. \quad (3)$$

The equations for the species b are obtained by replacing a with b and vice versa. We introduce the notation "θ" ($\theta = a, b$) in order to denote one of the species. Because of the axisymmetry, the velocity field of the gas "θ" ($\theta = a, b$) is: $\bar{\mathbf{u}}_\theta = \bar{u}_\theta(\bar{r}, \bar{z}) \mathbf{e}_r + \bar{v}_\theta(\bar{r}, \bar{z}) \mathbf{e}_z$. As well, ρ_θ is the volumetric mass, $\bar{\sigma}_\theta$ is the Navier-Stokes stress tensor of the species θ , $\bar{\mathbf{q}}_\theta$ is the heat flux vector and \bar{e}_θ is the specific internal energy. In addition to the usual equations, some coupling terms appear in the previous equations. These terms are derived from a BGK-type model for binary gas mixture (see for instance [4, 13, 6]). From this modeling we have:

$$\bar{\mathbf{u}}_a^* = \bar{\mathbf{u}}_b^* = \frac{m_a \bar{\mathbf{u}}_a + m_b \bar{\mathbf{u}}_b}{m_a + m_b}, \quad (4)$$

$$\bar{v}_{ab} = \bar{v}_a \left(\frac{d_a + d_b}{2 d_a} \right)^2 \left(\frac{m_a + m_b}{2 m_b} \right)^{\frac{1}{2}} \frac{\bar{n}_b}{\bar{n}_a} \psi_{ab}, \quad (5)$$

with:

$$\psi_{ab} = \left(\left(\frac{d_a}{d_b} \right)^2 \sqrt{\frac{m_b}{m_a} \frac{\Omega_b \bar{\mu}_a \bar{T}_b}{\Omega_a \bar{\mu}_b \bar{T}_a}} \right)^{1/2}, \quad (6)$$

where m_θ is the molecular mass of the species θ and where d_θ , \bar{v}_θ and \bar{n}_θ are respectively the molecular diameter, the collision frequency and the numerical density of the species θ . With these definitions, v_{ba} is obtained from v_{ab} by replacing "a" with "b" and the total number of collisions between species a and b is balanced:

$$\bar{n}_a \bar{v}_{ab} = \bar{n}_b \bar{v}_{ba}. \quad (7)$$

As a consequence, the conservation of the global momentum is satisfied. Additionally:

$$\bar{v}_\theta = \frac{\bar{p}_\theta}{\bar{\mu}_\theta} \Omega_\theta \quad \text{with} \quad \bar{\mu}_\theta = \mu_\theta^{ref} \left(\frac{\bar{T}_\theta}{T_\theta^{ref}} \right)^{\omega_\theta} \quad \text{and} \quad \Omega_\theta = \frac{5(\alpha_\theta + 1)(\alpha_\theta + 2)}{\alpha_\theta(7 - 2\omega_\theta)(5 - 2\omega_\theta)}, \quad (8)$$

where \bar{p}_θ is the pressure of the species θ , α_θ is a constant depending on the collision potential model and where ω_θ is the power exponent of the viscosity law (see [1, 4]). In the energy balance equation the coupling term may be expressed as:

$$\bar{S}_a^E = \frac{1}{2} \bar{\rho}_a \bar{v}_{ab} \left[\bar{\mathbf{u}}_a^{*2} - \bar{\mathbf{u}}_a^2 + \frac{2r_a}{\gamma_a - 1} (\bar{T}_a^* - \bar{T}_a) \right], \quad (9)$$

with $r_a = k/m_a$ where k is the Boltzmann constant and where \bar{T}_a is the temperature of the species a . In this expression, the temperature \bar{T}_a^* is given by a Morse formula [4] extended to polyatomic ideal gases:

$$\bar{T}_a^* = \bar{T}_a + \frac{3}{2} (\gamma_a - 1) \frac{2m_a m_b}{(m_a m_b)^2} \left(\bar{T}_b - \bar{T}_a + \frac{m_b}{6k} (\bar{\mathbf{u}}_b - \bar{\mathbf{u}}_a)^2 \right). \quad (10)$$

According to this definition and equation (7): $\bar{S}_a^E + \bar{S}_b^E = 0$ that coincides with total energy conservation. In addition, we have the ideal gas equations:

$$\bar{p}_\theta = r_\theta \bar{\rho}_\theta \bar{T}_\theta, \quad (11)$$

and the usual Fourier and Navier-Stokes constitutive laws. For the viscosity coefficients, we adopt the Stokes hypothesis. The first order wall boundary conditions are [7, 8]:

$$\bar{v}_\theta|_{\bar{r}=R} = \left(-\frac{\bar{\mu}_\theta \sigma_{\theta p}}{\bar{p}_\theta} \sqrt{2r_\theta \bar{T}_\theta} \frac{\partial \bar{v}_\theta}{\partial \bar{r}} + \frac{\sigma_{\theta T} r_\theta \bar{\mu}_\theta}{\bar{p}_\theta} \frac{\partial \bar{T}_\theta}{\partial \bar{z}} \right)_{\bar{r}=R}, \quad (12)$$

$$\bar{u}_\theta|_{\bar{r}=R} = 0, \quad (13)$$

$$\bar{T}_\theta|_{\bar{r}=R} = \bar{T}_w(\bar{z}) - \left(\xi_{\theta T} \sqrt{2r_\theta \bar{T}_\theta} \frac{\bar{\mu}_\theta}{\bar{p}_\theta} \frac{\partial \bar{T}_\theta}{\partial \bar{r}} \right)_{\bar{r}=R}, \quad (14)$$

where the constant coefficients $\sigma_{\theta p}$, $\sigma_{\theta T}$ and $\xi_{\theta T}$ characterize the viscous and thermal slip of the species θ on the walls [14]. The upstream and downstream boundary conditions for the pressures will be specified further.

In order to discuss the magnitude orders of the terms in the model equations, we write the corresponding dimensionless equations. We choose L as the longitudinal length scale and R as the radial length scale and we set $\epsilon = R/L \ll 1$. Additionally, the characteristic values of the radial and longitudinal velocities, the temperature, the pressure and the volumetric mass are respectively: U and V , T_c (for the two species), $p_{\theta c}$ and $\rho_{\theta c}$ (with $p_{\theta c} = r_\theta \rho_{\theta c} T_c$, $\theta = a, b$). With these characteristic scales, we built the following dimensionless numbers:

$$\gamma_a = \frac{c_{pa}}{c_{va}}, \quad Pr_a = \frac{\mu_a c_{pa}}{\kappa_a}, \quad Re_a = \frac{\rho_{ac} V L}{\mu_a}, \quad Ma_a = \frac{V}{\sqrt{\gamma_a r_a T_c}}. \quad (15)$$

Obviously, similar dimensionless numbers are built for the second species. Since Pr_θ is constant, μ_θ and κ_θ are both proportional to $T_\theta^{\omega_\theta}$. Now we are interested in the steady case. From the Principle of Least Degeneracy [15], we must keep the two terms in the dimensionless mass laws. Consequently $U = \epsilon V$. In order to investigate the significative degeneracies, we assume that the Reynolds number and that the Mach number are small or of order unity; we set $Re_a = R_a \epsilon^\alpha$ and $Ma_a = M_a \epsilon^\beta$ where both R_a and M_a are of order of the unity. The analysis of the magnitudes of the terms in the dimensionless balance laws derived from (1), (2) and (3) leads to a Mach number of order ϵ and to a Reynolds number of order unity that is to $\alpha = 0$ and $\beta = 1$ [13]. At the first approximation order, we have the following dimensionless equations:

$$\frac{1}{r} \frac{\partial}{\partial r} (r \rho_a u_a) + \frac{\partial}{\partial z} (\rho_a v_a) = 0, \quad (16)$$

for the mass. For the longitudinal and radial balance of momentum, we have:

$$0 = -\frac{1}{\gamma_a M_a^2} \frac{\partial p_a}{\partial z} + \frac{1}{R_a} \frac{1}{r} \frac{\partial}{\partial r} \left(r \mu_a \frac{\partial v_a}{\partial r} \right) + F_{ab} \frac{\rho_{bc}}{\rho_{ac}} \left(\frac{\mu_{ac}}{\mu_{bc}} \right)^{\frac{1}{2}} \frac{R_a}{\gamma_a M_a^2} p_a p_b \frac{(v_b - v_a)}{T(z)^{1 + \frac{\omega_a + \omega_b}{2}}}, \quad (17)$$

$$0 = -\frac{1}{\gamma_a M_a^2} \frac{\partial p_a}{\partial r}, \quad (18)$$

with:

$$F_{ab} = \left(\frac{m_b}{m_a}\right)^{\frac{1}{4}} \frac{m_a}{\sqrt{2 m_b(m_a + m_b)}} \left(\frac{d_a + d_b}{2 d_a}\right)^2 \frac{d_a}{d_b} \sqrt{\Omega_a \Omega_b}. \quad (19)$$

For the species a , the first order dimensionless energy balance equation is:

$$0 = \frac{\gamma_a}{R_a P r_a} \left[\frac{1}{r} \frac{\partial}{\partial r} \left(r \kappa_a \frac{\partial T_a}{\partial r} \right) \right] + G_{ab} \frac{R_a}{\gamma_a M_a^2} \frac{\rho_b p_a}{\sqrt{\mu_a \mu_b}} \sqrt{\frac{T_b}{T_a}} (T_b - T_a), \quad (20)$$

with:

$$G_{ab} = \frac{3 m_a (\gamma_a - 1)}{m_a + m_b} \frac{\rho_{bc}}{\rho_{ac}} \frac{\mu_{ac}}{\mu_{bc}} F_{ab}. \quad (21)$$

For the sake of simplicity, we do not write here the dimensionless equations for the other species but they are easily obtained by changing a in b and vice versa in the previous equations. First we consider the energy balance equation (20) and we assume that the two gases are in thermal equilibrium. In that case, the equation (20) with the boundary condition (14) admits a unique solution:

$$T_a(r, z) = T_w(z) = T_b(r, z) = T(z). \quad (22)$$

Finally, the dimensionless wall boundary conditions for the velocities are:

$$v_\theta(r=1, z) = -K_\theta \frac{[T_\theta(z)]^{\omega_a + \frac{1}{2}}}{p_\theta(z)} \frac{\partial v_\theta}{\partial r}(r=1, z) + \frac{\sigma_{\theta T}}{R_\theta} [T_\theta(z)]^{\omega_a} \frac{dT_\theta}{dz}(z), \quad u_\theta(r=1, z) = 0, \quad (23)$$

with: $K_\theta = \sigma_{\theta p} \sqrt{2\gamma_\theta} \frac{M_\theta}{R_\theta}$. At the first order, we obtain a set of six equations: the mass and the momentum equations for the two species. In the next section we will investigate the solution of this set of equations.

FIRST ORDER SOLUTION

The radial momentum equations (18) for the two species lead to pressures depending only on the longitudinal space variable z . If we use, in addition, the dimensionless ideal gas law, we have: $p_a(z) = \rho_a(z) T(z)$ and $p_b(z) = \rho_b(z) T(z)$. Consequently, the problem equations are reduced to:

$$\frac{1}{r} \frac{\partial}{\partial r} (r p_a u_a) + \frac{\partial}{\partial z} (p_a v_a) = 0, \quad (24)$$

$$\frac{1}{r} \frac{\partial}{\partial r} (r p_b u_b) + \frac{\partial}{\partial z} (p_b v_b) = 0, \quad (25)$$

$$\frac{1}{r} \frac{\partial}{\partial r} \left(r \frac{\partial v_a}{\partial r} \right) - \frac{B_a}{A_a} p_a p_b (v_a - v_b) = \frac{1}{A_a} \frac{dp_a}{dz}, \quad (26)$$

$$\frac{1}{r} \frac{\partial}{\partial r} \left(r \frac{\partial v_b}{\partial r} \right) + \frac{B_b}{A_b} p_a p_b (v_a - v_b) = \frac{1}{A_b} \frac{dp_b}{dz}, \quad (27)$$

with:

$$A_\theta = \frac{\gamma_\theta M_\theta^2}{R_\theta} [T_\theta(z)]^{\omega_\theta}, \quad \theta = a, b, \quad (28)$$

and:

$$B_a = R_a \frac{\rho_{bc}}{\rho_{ac}} F_{ab} \left(\frac{\mu_{ac}}{\mu_{bc}}\right)^{\frac{1}{2}} [T_a(z)]^{-(1 + \frac{\omega_a + \omega_b}{2})}, \quad B_b = R_b \frac{\rho_{ac}}{\rho_{bc}} F_{ba} \left(\frac{\mu_{bc}}{\mu_{ac}}\right)^{\frac{1}{2}} [T_b(z)]^{-(1 + \frac{\omega_a + \omega_b}{2})}. \quad (29)$$

In the expressions (28) and (29), A_a , A_b , B_a and B_b are functions depending on z . The longitudinal momentum equations (26) and (27) are solved to obtain the longitudinal velocities. They are the solutions of zero order modified

Bessel equations. Since the longitudinal velocities of the two gases must be finite at the channel axis ($r = 0$), the Bessel function of the second kind vanishes in the solutions. With the wall boundary conditions (23), these velocities can be expressed in terms of the pressures, of first kind modified Bessel function of order zero and one and in terms of non linear functions depending on z . Their detailed expressions are given in [5].

As a consequence of the mass balance equations, the pressure of each gas is given by an ordinary differential equation. In order to obtain these equations, we integrate the mass balance equations of each species (24) and (25) from $r = 0$ to $r = 1$. We use the wall boundary conditions for the transversal velocities and we obtain:

$$\int_0^1 \rho_a(z) v_a(r, z) r dr = \frac{Q_{ma}}{2}, \quad (30)$$

$$\int_0^1 \rho_b(z) v_b(r, z) r dr = \frac{Q_{mb}}{2}, \quad (31)$$

where Q_{ma} and Q_{mb} are the constant dimensionless mass flow rate of each species ($Q_{m\theta} = \bar{Q}_{m\theta}/(\rho_{\theta c} \pi R^2 V)$, $\theta = a, b$). The equations (30) and (31) are integrated in r to obtain two ordinary differential equations for the two pressures $p_a(z)$ and $p_b(z)$. For the sake of brevity, the detailed equations are not given here but they can be found in [5].

TABLE 1. Physical properties of the gases [1],

| | Argon | Neon | Xenon |
|------------------------|-----------------------|-----------------------|-----------------------|
| molecular mass (kg) | $66.3 \cdot 10^{-27}$ | $33.5 \cdot 10^{-27}$ | $218 \cdot 10^{-27}$ |
| molecular diameter (m) | $4.11 \cdot 10^{-10}$ | $2.72 \cdot 10^{-10}$ | $5.65 \cdot 10^{-10}$ |
| γ | 5/3 | 5/3 | 5/3 |
| μ_{VSS} (Pa.s) | $2.117 \cdot 10^{-5}$ | $2.975 \cdot 10^{-5}$ | $2.107 \cdot 10^{-5}$ |
| α | 1.40 | 1.31 | 1.44 |
| ω | 0.81 | 0.66 | 0.85 |

NUMERICAL SOLUTION

In order to solve the two pressure equations, the wall temperature and four boundary conditions are required: the inlet pressures p_a and p_b and the mass flow rates \bar{Q}_{ma} and \bar{Q}_{mb} for instance. In order to compare the asymptotic and DSMC approaches, we set the boundary conditions of the asymptotic model from a DSMC simulation. We set: $\bar{p}_a(-L/2) = 2.33 \cdot 10^4$ Pa, $\bar{p}_b(-L/2) = 2.64 \cdot 10^4$ Pa, $\bar{Q}_{ma} = 1.57 \cdot 10^{-13}$ kg.s⁻¹ and $\bar{Q}_{mb} = 8,21 \cdot 10^{-14}$ kg.s⁻¹. We consider the case of an isothermal flow ($T = 300$ K) of a mixing of Argon (a) and Neon (b). The physical properties of the gases are given in Tab. 1. These values are used in DSMC simulations with Bird's DS2V [16] as well as in the numerical integration of the asymptotic model. For the DSMC simulation, we set a diffuse boundary condition with full accommodation to the wall temperature and the VSS collision model is used [1].

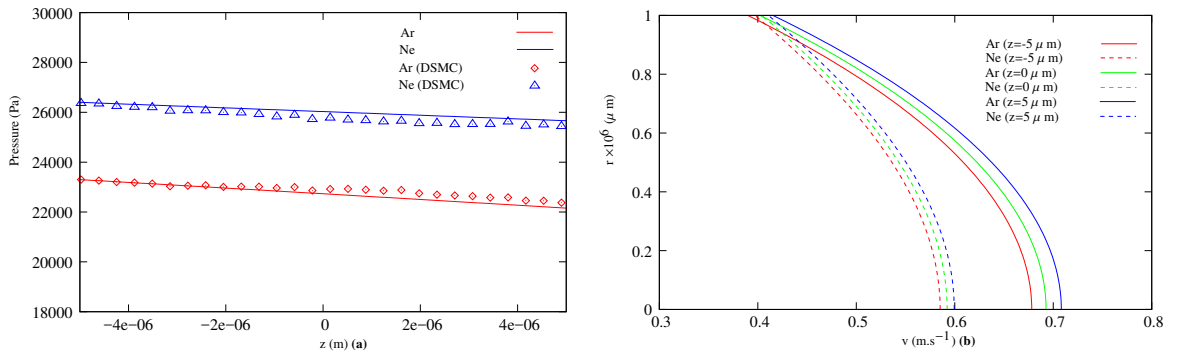


FIGURE 2. Pressures along the channel axis : comparison to DSMC (a) - Axial velocities (asymptotic model) (b)

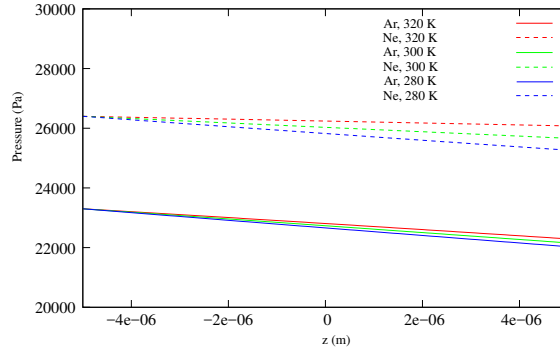


FIGURE 3. Pressures along the channel axis for $T_{in} = 300$ K and different values of T_{out}

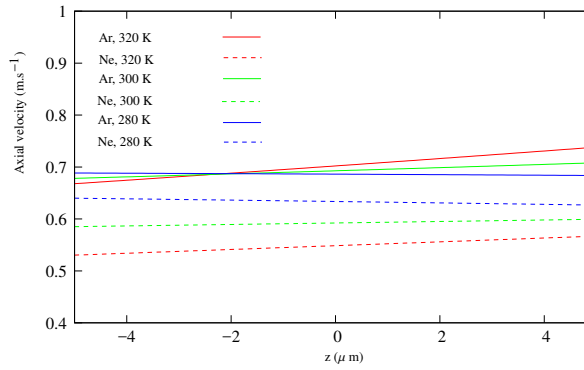


FIGURE 4. Axial velocities along the channel axis ($r = 0$) for $T_{in} = 300$ K and different values of T_{out}

The pressure equations are solved with MATLAB ; a fourth order Runge-Kutta method with variable stepsizes is used. With the pressures resulting from this short computation, the axial velocity of each species is calculated from their expression obtained from the momentum equations (26) and (27). The solution of the asymptotic model is compared to DSMC in Fig. 2a.

While DS2V needs a few days to produce a solution, only a few seconds are required for the asymptotic model. Even though latest DSMC programs are expected to be more efficient than Bird's DS2V, the computation time is strongly decreased for the asymptotic model. Figure 2a shows the evolution of the pressure along the channel axis for each gas. We have a good agreement between the DSMC simulation and the asymptotic solution. At the channel outlet, for instance, the difference between the pressures from the asymptotical approach and the DSMC simulation is about 1% for both gases. Since the pressure difference between the inlet and the outlet of the channel, for the two species, is weak, the pressures, in both calculations, seem to be quasi linear in z .

The difference between the asymptotical approach and the DSMC simulation is a consequence of the strong non linearity of the pressure equations: They are very sensitive to the boundary conditions. As a consequence, a small variation in the inlet pressure and in the mass flow rate leads to a great variation of the solution. In addition, these boundary conditions are obtained from DSMC simulations. Consequently, because of the numerical noise in the DSMC results, it is not easy to set the boundary conditions of the analytical set of equations at a convenient level of accuracy. Moreover, the statistical error for the velocities in DSMC computations is inversely proportional to the Mach number [17] which is of order $3 \cdot 10^{-3}$ in the present case. The result is an important DSMC error on the velocities (around 6%) and, consequently, on the mass flow rates. The evolution of the longitudinal velocities is plotted on Fig. 2b. In the case of two gases with identical molecular mass, the axial velocities of each species were very close [5]. In the present case, as a result of the molecular mass difference, the axial velocities of each species are very different. With the chosen boundary conditions, the two gases are accelerated along the channel and the axial

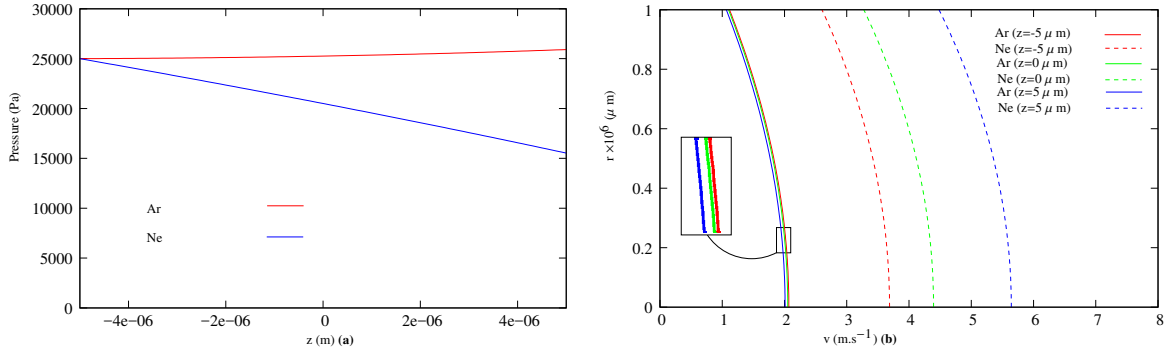


FIGURE 5. Ar-Ne mixture: Pressure along the channel axis (a) - Axial velocities (b)

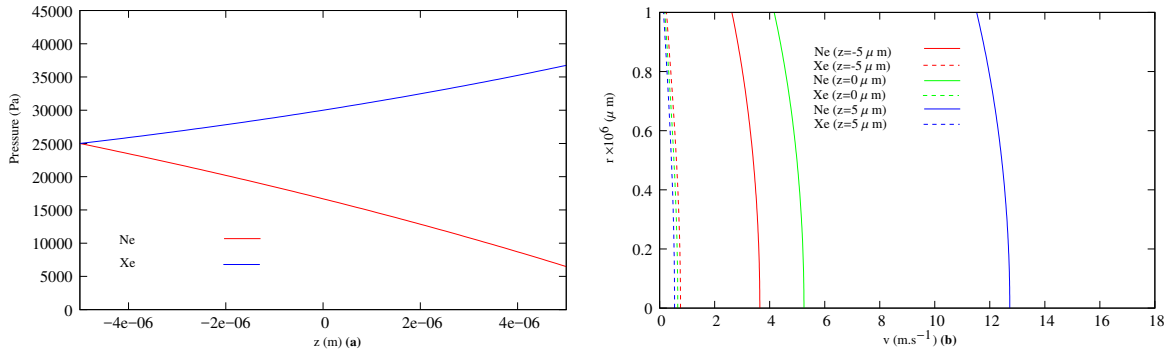


FIGURE 6. Xe-Ne mixture: Pressure along the channel axis (a) - Axial velocities (b)

velocity of Argon is greater than the axial velocity of Neon.

For the same gases, we focus on the effect of the constant gradient of temperature. The inlet temperature is still 300 K and we set different values of the outlet temperature. The inlet pressures and the mass flow rates are unchanged: $\bar{p}_a(-L/2) = 2.33 \cdot 10^4$ Pa, $\bar{p}_b(-L/2) = 2.64 \cdot 10^4$ Pa, $\bar{Q}_{ma} = 1.57 \cdot 10^{-13}$ kg.s⁻¹ and $\bar{Q}_{mb} = 8,21 \cdot 10^{-14}$ kg.s⁻¹. Figure 3 shows the evolution of the pressure of each species for three different outlet temperatures. The pressures decrease with z . For a given value of z , the pressures increase with the outlet temperature. This result is in agreement with the observations in the plane case [11] and in the case of gases with identical molecular mass [5]. The axial velocities along the channel axis ($r=0$) are plotted in Fig. 4. In the isothermal case ($T_{out} = 300$ K), as expected [12, 5], the longitudinal velocity increases along the channel as the pressure decreases. In the non isothermal cases, the effect of the thermal creep is observed. It induces a movement of the gases from the cold end of the channel to the hot one: when the inlet temperature is greater than the outlet temperature (case $T_{out} = 280$ K), the effects of the pressure gradient and of the temperature gradient are opposite and, as a consequence, we observe that the velocity decreases along the channel. When the inlet temperature is lower than the outlet temperature, (case $T_{out} = 320$ K), both the pressure and temperature gradients accelerate the gases along the channel.

Now we consider two different gas mixing: Ar/Ne and Ne/Xe. We set the following boundary conditions: $\bar{p}_a(-L/2) = \bar{p}_b(-L/2) = 2,5 \cdot 10^4$ Pa and $\bar{Q}_{ma} = \bar{Q}_{mb} = 5 \cdot 10^{-13}$ kg.s⁻¹. The channel wall is isothermal (300 K). The physical properties of the gases are given in Tab. 1. The numerical results are given in Fig. 5 and Fig. 6. In the two cases, the pressure of the heaviest species increases along the channel ; as a consequence, its axial velocity decreases along the channel. In contrast, the pressure of the lightest species decreases and, consequently, the gas is accelerated along the channel. The axial velocity of the heaviest species, because of a greater inertia, is less modified than the axial velocity of the lightest gas.

CONCLUSION

In this contribution, we present an original asymptotic study to analyze the flow of a gaseous mixture in a microchannel. The model is obtained from Navier-Stokes-Fourier equations with additional coupling terms. The longitudinal velocities are given explicitly in term of the pressures that are computed from a first order set of differential equations. The main advantage of this method, compared to DSMC simulations, is a very shorter computation time. As a consequence, the parametric studies are made easier.

The results have been compared to DSMC simulations and the two methods are in good agreement. The effect of a constant wall temperature gradient has been investigated: We observed the thermal creep. The case of gases with different molecular masses has been studied.

REFERENCES

- [1] G. A. Bird, "Gas dynamics and the direct simulation of gas flows," (Clarendon Press, 1994).
- [2] O. Aktas, N. R. Aluru, and U. Ravaioli, *J. Microelectromech. S.* **10**, 538–549 (2001).
- [3] S. Chapman and T. G. Cowling, "The mathematical theory of non-uniform gases," (C. U. P., 1952), pp. 278–294.
- [4] T. G. Elizarova, I. A. Graur, and J. C. Lengrand, *Eur. J. Mech. B-Fluids* **3**, 351–369 (2001).
- [5] C. Croizet and R. Gatignol, *AIP Conference Proceedings* **1786**, p. 080010 (2016).
- [6] R. Gatignol and C. Croizet, *Physics of Fluids* **29**, p. 042001 (2017), <http://dx.doi.org/10.1063/1.4979683> .
- [7] S. Kandlikar, S. Garimella, D. Li, S. Colin, and M. King, "Transfer and fluid flow in minichannels and microchannels," (Elsevier, 2005).
- [8] G. Karniadakis and A. Beskok, "Microflows - fundamentals and simulation," (Springer, 2006).
- [9] M. Reyhanian, C. Croizet, and R. Gatignol, *Mechanics and Industry* **14**, 453–460 (2013).
- [10] R. Gatignol and C. Croizet, "Asymptotic modelling of the flows in micro-channel by using macroscopic balance equation," in *Proceedings of the 27th Int. Symp. on Rarefied Gas Dynamics*, edited by A. Levin, I. J. Wysong, and A. L. Garcia (American Institute of Physics, New York, 2011), pp. 730–735.
- [11] R. Gatignol and C. Croizet, "Asymptotic modelling of the flow of a thermal binary gas mixture in a microchannel," in *Proceedings of the 28th Int. Symp. of Rarefied Gas Dynamics*, AIP Conference Proceedings (American Institute of Physics, New York, 2014), pp. 807–814.
- [12] C. Croizet and R. Gatignol, "Asymptotic modelling of the axisymmetric flow of a binary gas mixture in a circular microchannel," in *Proceedings of the 28th Int. Symp. of Rarefied Gas Dynamics*, AIP Conference Proceedings (American Institute of Physics, New York, 2014), pp. 799–806.
- [13] M. Reyhanian-Mashhadi, "Simulation numérique par la méthode de monte carlo (dsmc) et modélisation analytique d'un mélange gazeux dans un micro canal," Ph.D. thesis, Université Pierre et Marie Curie, Paris 2011.
- [14] F. Sharipov and V. Seleznev, *J. Phys. Chem. Ref. Data* **27**, 657–706 (1998).
- [15] M. Van Dyke, "Perturbation methods in fluid mechanic," (Academic Press, 1964).
- [16] G. A. Bird, "DSMC resources, <http://gab.com.au>," (2014).
- [17] N. Hadjiconstantinou, A. Garcia, and G. Bazant, *J. Comp. Phys.* **187**, 274–297 (2003).